

NEW SUB-MILLIMETER HETERODYNE OBSERVATIONS OF CO AND HCN IN TITAN'S ATMOSPHERE WITH THE APEX SWEDISH HETERODYNE FACILITY INSTRUMENT^a

M. RENGEL*, H. SAGAWA[†] and P. HARTOGH

*Max-Planck-Institut für Sonnensystemforschung,
Max-Planck-Straße 2, D-37191 Katlenburg-Lindau, Germany
rengel@mps.mpg.de*

The origin of the atmosphere of the largest moon of Saturn, Titan, is poorly understood and its chemistry is rather complicated. Ground-based millimeter/sub-millimeter heterodyne spectroscopy resolves line shapes sufficiently to determine information in Titan's atmospheric composition (on vertical profiles and isotopic ratios). We test the capabilities of the Swedish Heterodyne Facility Instrument (SHFI), Receiver APEX-1, together with the Atacama Pathfinder EXperiment APEX 12-m telescope for Titan's atmospheric observations. In particular, we present sub-millimeter observations of the CO(2-1) and HCN(3-2) lines of the Titan stratosphere with APEX, and with SHFI taken during the science verification (SV) instrument phase in March and June 2008. With the help of appropriate radiative transfer calculations, we investigate the possibility to constrain the chemical concentrations and optimize the performance of the APEX-1 instrument for inferring vertical profiles of molecular components of the atmosphere of Titan.

This study attempts to contribute to constrain radiative transfer and retrieval algorithms for planetary atmospheres, and to give hints to the current and future ground and space-based data acquisition leading to a more thorough understanding of the chemical composition of Titan.

1. Introduction

Titan's atmosphere exhibits a complex photochemistry. The origin of carbon monoxide (CO) is not well understood (whether photochemical or

^aBased on observations collected at the European Southern Observatory, Chile, corresponding to the observing proposal number 081.F-9812(A).

*Corresponding author.

[†]Currently at the National Institute of Information and Communications Technology, Japan.

primordial). Hydrogen cyanide (HCN), the most abundant nitrile in Titan, is a key intermediate in production of more complex hydrocarbons and organic molecules. HCN in the Titan atmosphere has been discovered by the infrared observations of Voyager 1,¹ and CO has been detected by the ground-based near-infrared observations.² Following these detections, the molecular concentrations of CO and HCN in Titan's atmosphere have been determined from infrared, millimeter, and sub-millimeter observations as well as from modeling (see Tables 2 and 3 in Section 4 for details). CO seems to be uniformly mixed in Titan's atmosphere up to high altitudes. HCN abundances, however, display a steeper profile with ambiguous enrichment values (Table 3). Already several observational data confirm that Titan's atmospheric composition is indeed seasonally^{3,4} and spatially dependent.⁵ Full behavior of the seasonal characteristics of the spatial distribution is not constrained yet due to the limitation in the temporal coverage of the previous observations and to the use of different instruments. New sub-millimeter observations are required not only to provide new abundance constraints and shed more light on the rate of these seasonal variations, for example, but for support, complement, and cross-calibration the ESA's Herschel space observatory mission. One of the goals of the key program of Herschel, entitled *Water and Related Chemistry in the Solar System*,⁶ is to understand water inventory in the Titan's atmosphere as well as distributions of other hydrocarbons and nitriles. During the guaranteed time, line surveys on Titan at the frequency range of 500 and 5000 GHz are going to be carried out using two low-to-medium resolution spectrometers (Photodetector Array Camera and Spectrometer (PACS) and Spectral and Photometric Imaging Receiver (SPIRE)). Our model calculations of the synthetic spectra of Titan expected to be observed with Herschel show that several CO and HCN lines will be detected with PACS and SPIRE.⁷ Because of their low-to-medium spectral resolutions, SPIRE and PACS are not capable of measuring the shapes of CO and HCN lines, which prevents us from determining precisely the vertical profile of CO and HCN mixing ratios. Therefore, high spectral resolution observations of CO and HCN with ground-based sub-millimeter telescopes would significantly improve the accuracy of retrieving the CO and HCN profiles.

The Atacama Pathfinder EXperiment (APEX) 12-m telescope is operational since 2005⁸ and has been already used to the planetary science (monitoring mesospheric winds of Venus⁹), among numerous galactic and extra-galactic objects. In spring 2008, the new APEX Swedish heterodyne facility instrument (SHFI) has been commissioned on the APEX 12-m

telescope,^{10,11} which consists of four single-pixel receivers (APEX-1, APEX-2, APEX-3, and APEX-T2) mounted in a single cryostat located in the Nasmyth A cabin of APEX. In this report, we present a summary of our observations of CO and HCN performed with APEX-1 during the science verification (SV) phase with the aims to demonstrate the capabilities of APEX and SHFI for Titan’s atmospheric observations and to investigate the possible retrieval of CO and HCN abundances. We also examine the possible detection of the millimeter/sub-millimeter rotational transition of C₂H₂ (already observed in the mid-infrared spectra by the Composite Infrared Spectrometer, CIRS, on Cassini¹²), and the search for one new compound, HC₅N(83-82) which the possible presence has been suggested by experimental results simulating Titan’s atmosphere.^{13–15}

The observations are described in detail in Section 2 while the radiative transfer modeling and the data analysis are discussed in Sections 3 and 4, respectively. A brief discussion is given in Section 5 and a summary in Section 6.

2. Observations

Titan’s spectra were acquired with the APEX 12-m telescope located on Chajnantor (Chile) during March 21 and June 17–18, 23, and 27, 2008 during SV. We used the APEX-1 receiver, operating at 211–270 GHz, which employs a superconductor–insulator–superconductor (SIS) mixer and behaves as a single-sideband receiver (SSB). For the backend, we used the fast Fourier transform spectrometer (FFTS) with a channel separation of 122 kHz and a bandwidth of 1 GHz. Table 1 summarizes the measured transitions as well as the observing days and the precipitable water vapor (PWV). Titan was observed near the western or eastern elongations at separation angles from Saturn greater than 120′. Pointing and focusing of

Table 1. Species observed on Titan.

Species	Frequency (GHz)	Date 2008	PWV (mm)
HCN(3-2)	265.886	21 March	
HC ₅ N(83-82)	220.937	17–18 June	3.5–4.0
CO(2-1)	230.538	23 June	0.5
HCN(3-2)	265.886	23 June	0.5
C ₂ H ₂ $J = 47 \nu 5 = 1 \rightarrow$ $J = 46 \nu 4 = 1$	254.521	27 June	0.2

the telescope were regularly checked scanning across Saturn in azimuth and in elevation (APEX has a pointing accuracy of $2''$ r.m.s. over sky). The apparent diameter of Titan was around $0.8''$.

Because a bug in the low-level Python ephemerides software not previously detected, Titan was not tracked properly at the beginning of our observations on March 21, 2008. The bug was successfully removed by the APEX staff. These observations, in particular, have helped to improve the control software. Accounting for possible frequency errors in the line center (of a few MHz around the respective line centers) and considering the short integration time, we could not detect any evident signature of HC_5N (83-82) and C_2H_2 in the recorded spectra averages of integration times of 36 and 91 min (r.m.s. of 0.035 and 0.03 K), respectively. Lower r.m.s. noise levels of around 0.01 K (which could be achieved with integration times of around 8 and 13 h, respectively) would have facilitated the possible detections of these species. Therefore, we concentrate here on the CO(2-1) and HCN(3-2) observations. Because of the high oversubscription of observing proposals and the uncertainties about the tracking at the beginning of the campaign, the initially proposed integration time of around 2 h for CO(2-1) and 2.65 h for HCN(3-2), which corresponds to a r.m.s. noise level of 0.017 K and 0.025 K respectively, was not available. Instead, CO(2-1) and HCN(3-2) were integrated for around 13 and 19 min, respectively. The initial reduction of each spectrum was performed using the CLASS software package of the Grenoble Astrophysics Group.^b

Figure 1 presents the recorded Titan's spectra of the CO(2-1) and HCN(3-2) lines. The resolution has been downgraded to about 4 MHz in order to increase the signal-to-noise ratio.

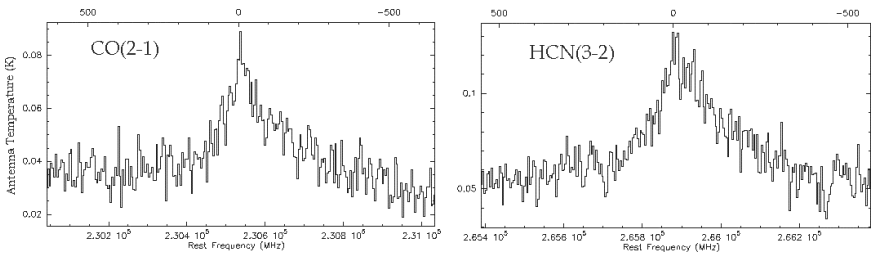


Fig. 1. Titan's spectra observed with the APEX 12-m Telescope on June 23, 2008. Left: CO(2-1) line rebinned over 32 resolution elements (4 MHz). Right: HCN(3-2) line rebinned over 32 resolution elements (4 MHz).

^bURL: <http://www.iram.fr/IRAMFR/GILDAS>.

The conversion from the observed antenna temperature T_a^* to the total flux density from the Titan's atmosphere $S_{\nu,\text{tot}}$ [Jy] is performed by $S_{\nu,\text{tot}} = 24.4 \times T_a^* \cdot \eta_f / \eta_a$, where η_f and η_a are the forward and aperture efficiencies, respectively. In this study, we adopt the values considering the efficiencies listed on the APEX Web site^c and of the instrument paper⁸: η_a are 39.9 and 40.2 for 230 and 265 GHz, respectively and η_f is 0.95 for both frequencies. These values are expected to have a 10% uncertainty.

By fitting the synthetic spectra to the observed one, we intend to infer the abundance of CO and HCN in Titan's stratosphere. A precise comparison of the observations with synthetic spectra must cope with two limitations: (1) the line-to-continuum ratios of these CO and HCN spectra were not able to be confirmed from the observed data. 1 GHz bandwidth is too narrow for constraining the continuum level. We have examined the possibility of using the emission at the frequency of ± 500 MHz offset from the line center as the pseudo-continuum. We found, however, that the intensities of the CO (2-1) line at the ± 500 MHz significantly depend on the CO abundance at a certain range of altitude, which also affects the intensity at the line center. Therefore, we conclude that using such fluxes as the pseudo-continuum is not a suitable method for determining the CO abundance in this study. This is also the case for the HCN (3-2) line. (2) Baseline ripples and uncorrected larger scale baseline characteristics may affect the shape of the observed spectra. One can obtain a spectral line shape symmetric with respect to the line center by folding the spectrum. However, such a spectra folding may introduce an artificial error in the line shape. Therefore, we prefer to keep the spectra with their original baseline distortions.

3. Radiative Transfer Modeling

The synthetic spectra are generated by a multi-layered line-by-line radiative transfer model considering the spherical geometry of Titan's atmosphere. It consists of 120 layers that span the 0–600 km interval with a resolution of 5 km. In general, the atmospheric model for Titan is explained fully in Rengel *et al.*⁷ Briefly, Titan's thermal and pressure profiles based on the *in-situ* measurement by the Huygens probe¹⁶ are adopted for the opacity calculation of the CO and HCN gases at each altitude level. The mixing

^cURL: <http://www.apex-telescope.org/telescope/efficiency/>.

ratio profiles of CO and HCN are set as the parameters to be retrieved in this study. The detail of modeling vertical profiles of each molecule is described later. For CO, the assumed N₂-broadening line-width here is that of Semmoud-Monnanteuil and Colmont,¹⁷ and for HCN, the value corresponding to the same transition at the infrared vibrational-rotational band¹⁸ as there is no exact measurement for this pure rotational line. The collision-induced absorption coefficients of N₂, CH₄, and H₂ mixtures, which dominate the millimeter and sub-millimeter continuum opacity of Titan's atmosphere, are included by using the formulation of Courtin¹⁹ and Borysow and Tang.²⁰

4. Data Analysis

4.1. The CO abundance

Recent observations suggest that CO in Titan is uniformly mixed throughout Titan's atmosphere.²¹⁻²³ Such a profile can be supported if its long chemical lifetime in the oxygen-poor Titan atmosphere is considered ($\sim 10^{-9}$ years²⁴). In this study, we retrieve CO abundance by assuming a vertically constant profile. It should be noted that some of the previous observations have shown the possibility of existence of the discontinuity in the CO mixing ratios between the troposphere and the stratosphere (e.g., ~ 30 ppm in the troposphere²⁵ and ~ 60 ppm in the stratosphere²⁶). However, such discontinuity cannot be constrained by our observations, as the CO(2-1) measurement reported here does not have any sensitivity to the altitude below 60 km (Fig. 2, left panel).

A direct comparison of synthetic and observed spectra is made and the best fitting model with the least χ^2 is determined. In Fig. 2 right panel, the best-fit CO abundance shows a solution of 30_{-8}^{+15} ppm. Although this solution agrees with the previous stratospheric CO measurements of Hidayat *et al.*²⁷ Lellouch *et al.*²⁵ and Baines *et al.*²² (Table 2), we have to allow a larger error on our result by considering the uncertainty in the flux scaling and the baseline problems. To examine the effect of the uncleaned baseline of the observed spectrum, we performed the fitting analysis by constraining the data only on each side of the wings. Using the red-shift wing ($\nu < \nu_0$) yielded the best fitting CO mixing ratio of 26_{-8}^{+13} ppm, while using the blue-shift wing ($\nu > \nu_0$) resulted 36_{-11}^{+15} ppm. Taking into account the 10% uncertainty in the flux calibration, the acceptable range of CO mixing ratio becomes as 16–51 ppm. This wide range covers most of the past works. One way to avoid such a large ambiguity in the data analysis (i.e., to avoid the effect of

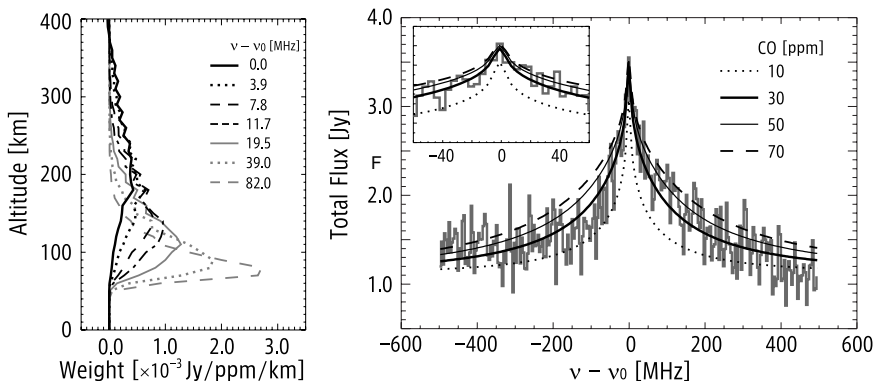


Fig. 2. Left: Weighting functions with respect to CO mixing ratio for selected frequencies near the CO(2-1) line center. Note that the finite spectral resolution (4 MHz) of the measurement is taken into account for the calculation of these weighting functions. Right: Observed and synthetic CO(2-1) spectra at 230.54 GHz (gray spectrum and line ones, respectively). The synthetic spectra are calculated assuming vertically uniform CO mixing ratios of 10, 30, 50, and 70 ppm (from bottom to top) respectively. The small upper panel shows a zoom of the spectrum for a frequency range of ± 60 MHz.

the uncertainty in the flux calibration) is to calibrate the observed spectrum by scaling its continuum level to that of the forward model calculation. Our forward model calculations suggest that the intensity at the frequency offset larger than ~ 1.5 GHz can be used as the continuum level.

4.2. The HCN vertical profile

We retrieve the mixing ratio profile of HCN by performing forward and inversion calculations iteratively. For solving the inversion problem, we employ the optimal estimation method (OEM) (e.g., see details in Rodgers³⁶). The Levenberg-Marquardt scheme is used in the iteration. We set the logarithm of HCN mixing ratio as the retrieving parameter. The *a priori* profile of HCN mixing ratio, which is required in the OEM approach to regularize the ill-posed inversion problem, is based on the previous ground-based work by Marten *et al.*³⁷ We assumed the *a priori* error of 2.3 in the logarithm scale. During the HCN retrieval, the temperature profile is fixed to our nominal temperature profile (the one based on the Huygens measurements).

Figure 3 shows the best-fit synthetic spectrum (solid line) and the corresponding HCN profile. The averaging kernels of the retrieved HCN

Table 2. Observations of CO in Titan atmosphere.

Altitude	Mixing ratio [ppm]	Wavelength* [μm]	Facility/Instrument	Reference
Troposphere	48^{+100}_{-32}	1.57	KPNO-4m/Fourier transform interferometer	2
Stratosphere	30–180	35314.89	VLT-70m/27 antennas	28
Stratosphere	60 ± 40	2602.59	OVRO/2 elements interferometers	29
Stratosphere	2^{+2}_{-1}	2602.59	IRAM-30m/3-mm SIS receiver	30
Stratosphere	50 ± 10	2602.59	OVRO/6 10.4 m diam. antennas	31
Troposphere	10^{+10}_{-5}	4.8	UK IR Telescope/CGS4 spectrograph	32
Stratosphere	27 ± 5	2602.59, 1304.34, 900.9	IRAM-30m/SIS heterodyne receivers	27
Stratosphere	52 ± 6	1304.34	OVRO/6 antennas	33
Troposphere	32 ± 10	4.75–4.85	VLT 8-m/ISAAC	25
Stratosphere	51 ± 4	869.56	SMA/5 and 6 antennas	21
153–350 km	60	4.5–4.85	VLT 8-m/ISAAC	26
Tropo-Stratosphere	45 ± 15	4.64	Cassini/CIRS	34
Stratosphere	32 ± 15	4.64	Cassini/VIMS	22
Stratosphere	47 ± 8	333.3–166.66	Cassini/CIRS	35
Stratosphere	30^{+15}_{-8}	1301.29	APEX/APEX-1 receiver	This article

*In spite that each wavelength region is defined by standard specific units, we use here μm to facilitate the comparisons.

mixing ratios indicate that this retrieval has a significant sensitivity at the altitude around 90 km though we can still retrieve information at the higher altitudes up to 240 km. Our retrieved HCN mixing ratios are larger than those of Marten *et al.*³⁷ by a factor of ~ 30 –80% at the altitudes of 100–200 km. The synthetic spectrum calculated with the *a priori* HCN profile, i.e., the result of Marten *et al.*³⁷ is also shown for comparison (Fig. 3). A large discrepancy between the observed and the synthetic spectra and the *a priori* profile are seen mostly at the wings of the spectrum. This results in the retrieved larger HCN abundances at the altitudes of 90–150 km. Note that our result showing lower HCN abundance values at around 300 km is out of the altitude range where our observations are sensitive.

In the above-mentioned retrieval, we only took the system temperature of the APEX-1 instrument into account for the statistical error of the measurement. In fact, as we discussed in Section 4.1, the observed spectrum

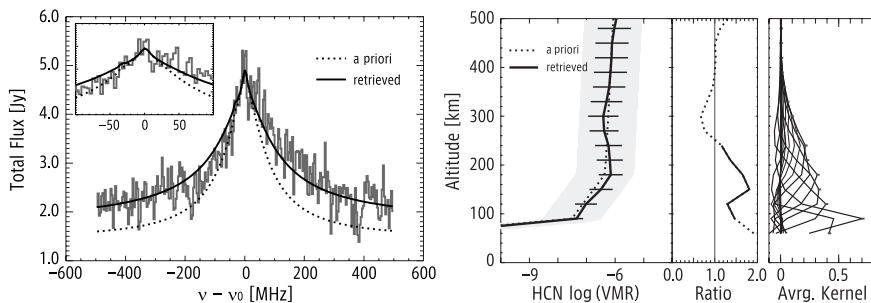


Fig. 3. Left: Observed and synthetic HCN(3-2) spectra at 265.89 GHz. Solid line shows the best-fit spectrum and dashed line shows the spectrum calculated with the *a priori* HCN profile. Gray line is the observed data. The upper panel figure represents the zoom to the frequency range of ± 100 MHz. Right: The retrieved HCN vertical profile (solid line) under the nominal temperature profile without considering the error in the flux calibration. The error bar indicates the $1\text{-}\sigma$ limit of the retrieval. The dotted profile represents the *a priori* values where the gray-shaded region corresponds to their errors. The ratio of the retrieved profile with respect to the *a priori* profile is also shown. On the extrem right panel, the averaging kernels of the retrieved HCN mixing ratios are shown.

contains the 10% uncertainty in the flux calibration. If a 10% larger scaling factor is applied in the flux calibration, we cannot derive any realistic HCN profiles, which can reproduce the observed spectrum. In case of using a 10% smaller scaling factor, the HCN abundances for the best-fit spectrum are larger than those of Marten *et al.*³⁷ at the altitude of 100–150 km (which is attributed by the wings of the spectrum) and then becomes as small as $\sim 30\%$ of Marten *et al.*³⁷ at higher altitudes of 150–200 km (Fig. 4).

The two retrievals (Figs. 3 and 4) demonstrate the significant impact of the flux calibration uncertainty on the retrieved HCN profile. Since we cannot constrain the line-to-continuum ratio of the observed spectrum, we

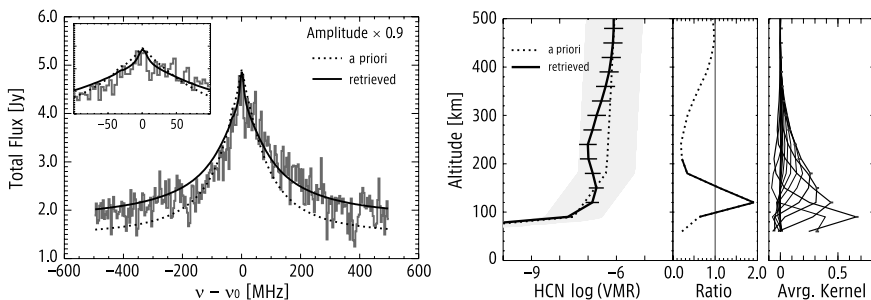


Fig. 4. See caption Fig. 3, but here the measurement data is scaled by a factor of 0.9.

are not able to conclude the HCN abundance at altitude of 150–200 km, which deviates within a wide range from 30 to 150% of the *a priori* guess. For the lower altitudes such as 100–150 km, the wing of our observed spectrum requires a higher opacity of HCN than that of Marten *et al.*³⁷ even if we consider the uncertainty in the flux calibration.

5. Discussion

How does one explain the behavior of the retrieved HCN vertical profile obtained here? The relative poor signal-to-noise of the observations obtained here results in a poor fit to the HCN line wings. Furthermore, comparing the results obtained with previous results derived from disk-averaged information, interferometer measurements, and space-based observations summarized in Table 3 must be considered cautiously. In other words, direct

Table 3. HCN mixing ratios in Titan’s atmosphere.

Altitude	Mixing ratio [ppm]	Wavelength* [μm]	Facility/ Instrument	Reference
Stratosphere	3.0×10^{-7}	3386.0	IRAM-30m/SIS receiver	38
Stratosphere	1.6×10^{-7}	14.025	Voyager/IRIS	39
Stratosphere	$(0.75-52) \times 10^{-7}$	3386.0	IRAM 30-m/SIS receiver	40
Stratosphere	$4.7 \times 10^{-8}-1.5 \times 10^{-6}$	14.025	Voyager/IRIS	41
400 km	$\sim 2 \times 10^{-5}$		Model prediction	42
Stratosphere	$(0.5-4) \times 10^{-7}$	14.025	IRAM 30-m/SIS receiver	43
400 km	1×10^{-6}		Model prediction	44
700 km	1×10^{-5}		Model prediction	44
400 km	1×10^{-6}	3386.0	IRAM-30m/SIS receiver	45
400 km	1×10^{-5}		Model prediction	46
700 km	1×10^{-4}		Model prediction	46
Stratosphere	3.0×10^{-7}	14.025	ISO/SWS	47
~ 600 km	7×10^{-3}	3	Keck II/ NIRSPEC	46
83 km	3×10^{-5}	1692.43	SMA/5 and 6 antennas	21
300 km	3×10^{-5}	1692.43	SMA/5 and 6 antennas	21
500 km	0.4×10^{-6}	14.04	Cassini/CIRS	48

*In spite that each wavelength region is defined by standard specific units, we use here μm to facilitate the comparisons.

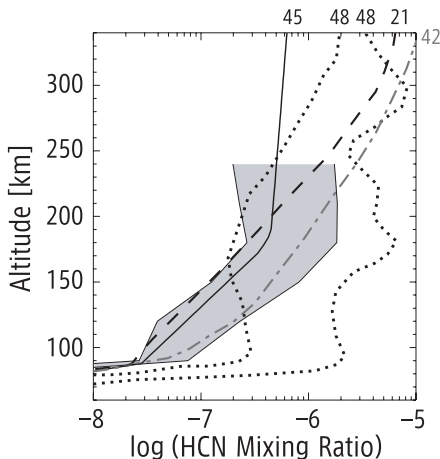


Fig. 5. Comparison of recent observational and modeling works of HCN abundances. The small numbers correspond to the indices of the reference on Table 3. The shaded region represents the results here obtained, considering the $1\text{-}\sigma$ limit of the retrieval error.

comparison of the results from different instruments requires us to assume that all instrument-related offsets have been accounted for.

Certainly, Titan's atmospheric temperature and composition are not in a steady state. Does the HNC abundance retrieved here perhaps indicate that the composition of Titan's atmosphere has changed during the last years? Figure 7 in Teanby *et al.*⁵ shows that the HCN abundance measured by Cassini (at southern latitudes) has not significantly changed between 2006 and 2008. Then, it seems to be that possible detections of time variations (if any) between different observations could be maybe due to observing more of the northern hemisphere than of the southern one as Titan's season changes. As we derived disk-averaged information, we need to keep in mind, however, that our vertical distributions are mostly representative of the equatorial region of Titan since the measured flux density spectra are more heavily weighted toward equatorial latitudes. In case that vertical distributions would be representative of the northern latitudes, the profile analysis would become rather complicated. There is evidence of a vortex, which acts to separate enriched from unenriched air, at $25\text{--}55^\circ\text{N}$ encircling the North Pole.^{5,34,49}

Further higher signal-to-noise HCN observations at different times are necessary in order to open the possibility to detect seasonal and even spatial variations in HCN, and confirm or not an enrichment layer in Titan's stratosphere.

6. Summary

- We report the first observations obtained with the SFHI APEX-1 instrument on APEX on a planetary/satellite atmosphere taken during SV. It consists of the spectra of CO(2-1) and HCN(3-2) in Titan's atmosphere.
- The observations reported here improved the control software of the APEX telescope, so that now it is possible to track planets with the APEX-1 receiver.
- We investigate the CO and HCN composition of Titan's stratosphere. Our CO mixing ratio estimation is consistent with other authors. We retrieved the HCN vertical profile, which is inconsistent with previous analyses. This requires further investigation by future HCN observations with higher signal-to-noise ratios. The search of nitriles and CO appears favorable in the sub-millimeter range explored with the APEX telescope and with the APEX-1 receiver.

This work represents a first step in exploring the capabilities of APEX and SHFI for Titan's atmospheric observations. New simultaneous observations of HCN and its isotopes at higher frequencies with APEX-2 and APEX-T2, for example, would improve the sensitivity to the abundance retrievals, and potentially could support, complement, and cross-calibrate the ESA's Herschel Space Observatory mission.

Acknowledgments

We are grateful to the APEX staff, in particular to Carlos De Breuck (ESO), for its assistance. We thank the anonymous reviewers for their constructive comments. This publication is based on data acquired with the Atacama Pathfinder Experiment (APEX). APEX is a collaboration between the Max-Planck-Institut für Radioastronomie, the European Southern Observatory, and the Onsala Space Observatory.

References

1. R. Hanel, *et al.*, *Science* **212** (1981) 192.
2. B. L. Lutz, C. de Bergh and T. Owen, *Publ. Astron. Soc. Pac* **95** (1983) 593.
3. H. G. Roe, I. de Pater and C. P. McKay, *Icarus* **169** (2004) 440.
4. N. A. Teanby, *et al.*, *Icarus* **193** (2008) 595.
5. N. A. Teanby, *et al.*, *Phil. Trans. R. Soc. A* **367** (2009) 697.

6. P. Hartogh, *et al.*, *Planet. Space Sci.* **57** (2009) 1596.
7. M. Rengel, H. Sagawa, and P. Hartogh, *Adv. Geo.* **19** (2010) 335–348.
8. R. Güsten, *et al.*, *Astron. Astrophys.* **454** (2006) L13.
9. E. Lellouch, *et al.*, *Planet. Space Sci.* **56** (2008) 1355.
10. V. Vassilev, *et al.*, *Astron. Astrophys.* **490** (2008) 1157.
11. O. Nyström, *et al.*, *J. Infrared Millimeter Terahertz Waves* **30** (2009) 746.
12. S. Vinatier, B. Bézard and C. A. Nixon, *Icarus* **191** (2007) 712.
13. E. de Vanssay, *et al.*, *Planet. Space Sci.* **43** (1995) 25.
14. P. Coll, *et al.*, *Adv. Space Res.* **16** (1995) 93.
15. A. Coupeaud, *et al.*, Laboratory study of the Titan's atmosphere chemistry: Formation and characterization of HC₅N, in *IAU Symposium*, IAU Symposium Vol. 235 (Cambridge University Press, California, August 2005).
16. M. Fulchignoni, *et al.*, *Nature* **438** (2005) 785.
17. N. Semmoud-Monnanteuil and J. M. Colmont, *J. Mol. Spec.* **126** (1987) 210.
18. M. A. H. Smith, *et al.*, *J. Mol. Spec.* **105** (1984) 105.
19. R. Courtin, *Icarus* **75** (1988) 245.
20. A. Borysow and C. Tang, *Icarus* **105** (1993) 175.
21. M. A. Gurwell, *Astrophys. J. Lett.* **616** (2004) L7.
22. K. H. Baines, *et al.*, *Planet. Space Sci.* **54** (2006) 1552.
23. R. de Kok, *et al.*, *Icarus* **186** (2007) 354.
24. Y. L. Yung, M. Allen and J. P. Pinto, *Astrophys. J. Suppl.* **55** (1984) 465.
25. E. Lellouch, *et al.*, *Icarus* **162** (2003) 125.
26. M. A. López-Valverde, E. Lellouch and A. Coustenis, *Icarus* **175** (2005) 503.
27. T. Hidayat, *et al.*, *Icarus* **133** (1998) 109.
28. D. O. Muhleman, G. L. Berge and R. T. Clancy, *Science* **223** (1984) 393.
29. G. Paubert, D. Gautier and R. Courtin, *Icarus* **60** (1984) 599.
30. A. Marten, *et al.*, *Icarus* **76** (1988) 558.
31. M. A. Gurwell and D. O. Muhleman, *Icarus* **117** (1995) 375.
32. K. S. Noll, *et al.*, *Icarus* **124** (1996) 625.
33. M. A. Gurwell and D. O. Muhleman, *Icarus* **145** (2000) 653.
34. F. M. Flasar, *et al.*, *Science* **308** (2005) 975.
35. R. de Kok, *et al.*, *Icarus* **186** (2007) 354.
36. C. D. Rodgers, *Rev. Geophys. Space Phys.* **14** (1976) 609.
37. V. N. Markov, *et al.*, *J. Mol. Spec.* **212** (2002) 1.
38. G. Paubert, *et al.*, *Bull. Am. Astron. Soc.* **19** (1987) 633.
39. A. Coustenis, B. Bézard and D. Gautier, *Icarus* **80** (1989) 54.
40. L. Tanguy, *et al.*, *Icarus* **85** (1990) 43.
41. A. Coustenis and B. Bézard, *Icarus* **115** (1995) 126.
42. L. M. Lara, *et al.*, *J. Geophys. Res.* **101** (1996) 23261.
43. T. Hidayat, *et al.*, *Icarus* **126** (1997) 170.
44. S. Lebonnois, *et al.*, *Icarus* **152** (2001) 384.
45. A. Marten, *et al.*, *Icarus* **158** (2002) 532.
46. T. R. Geballe, *et al.*, *Astrophys. J. Lett.* **583** (2003) L39.
47. A. Coustenis, *et al.*, *Icarus* **161** (2003) 383.
48. N. A. Teanby, *et al.*, *Icarus* **186** (2007) 364.
49. R. K. Achterberg, *et al.*, *Icarus* **194** (2008) 263.